JKAU: Eng. Sci., **vol. 11 no. 1,** pp. 119-141 (1419 A.H. / 1999 A.D.)

Mathematical Modeling of Solar Operated Liquid Desiccant, Evaporative Air Conditioning System

A.M. RADHWAN*, M.M. ELSAYED**, H.N. GARI*
**Mechanical Eng. Dept., King Abdulaziz University, Saudi Arabia*
***Mechanical Engineering Dept., Kuwait University, Kuwait*

ABSTRACT. A solar operated liquid desiccant ($CaCl_2$), evaporative air conditioning system is mathematically modeled. Several modifications were introduced to improve the system performance. Three indices; desiccant replacement factor *DRF*, system thermal ratio *STR* and solar utilization factor *SUF* were defined to evaluate the system performance at various operating conditions. The long term system performance at the weather conditions of Jeddah, Saudi Arabia is investigated and also the effect of varying solar collector area and the height of the proposed thermal storage tank are studied in terms of *DRF*, *STR* and *SUF*. It is found that the monthly-averaged daily value of *DRF* is highest during the summer while the lowest value occurs in the winter. *SUF* shows an opposite behavior to *DRF*. The monthly variation of the efficiency and *STR* vary slightly during the seasons. These results showed that the system performance is good at humid weather conditions.

1. Introduction

In hot weather conditions, air conditioning is strongly needed. Fortunately, in those hot regions solar energy is abundant and free for long periods of the year. Research on using solar energy for cooling systems has started in the fifties[1-3]. Recently, solar cooling systems using desiccant materials have been analyzed, investigated and experimented[4-14]. Solar energy is utilized for the reconcentration (regeneration) of liquid desiccant because of its suitability for the required range of temperature (50-60ºC).

In the present work, an integrated desiccant-vapor compression air conditioning system, Fig. 1, is considered. A mathematical model is prepared for the simulation of heat and mass transfer processes in packed beds, air washers, solar air heaters, rock bed thermal storage and other system components. A computer program package is prepared and tested using the model to predict the system performance at various parametric conditions in terms of *DRF*, *STR* and *SUF*. The effect of weather conditions, solar collector area and the height of the rock bed thermal storage on the system performance have been studied.

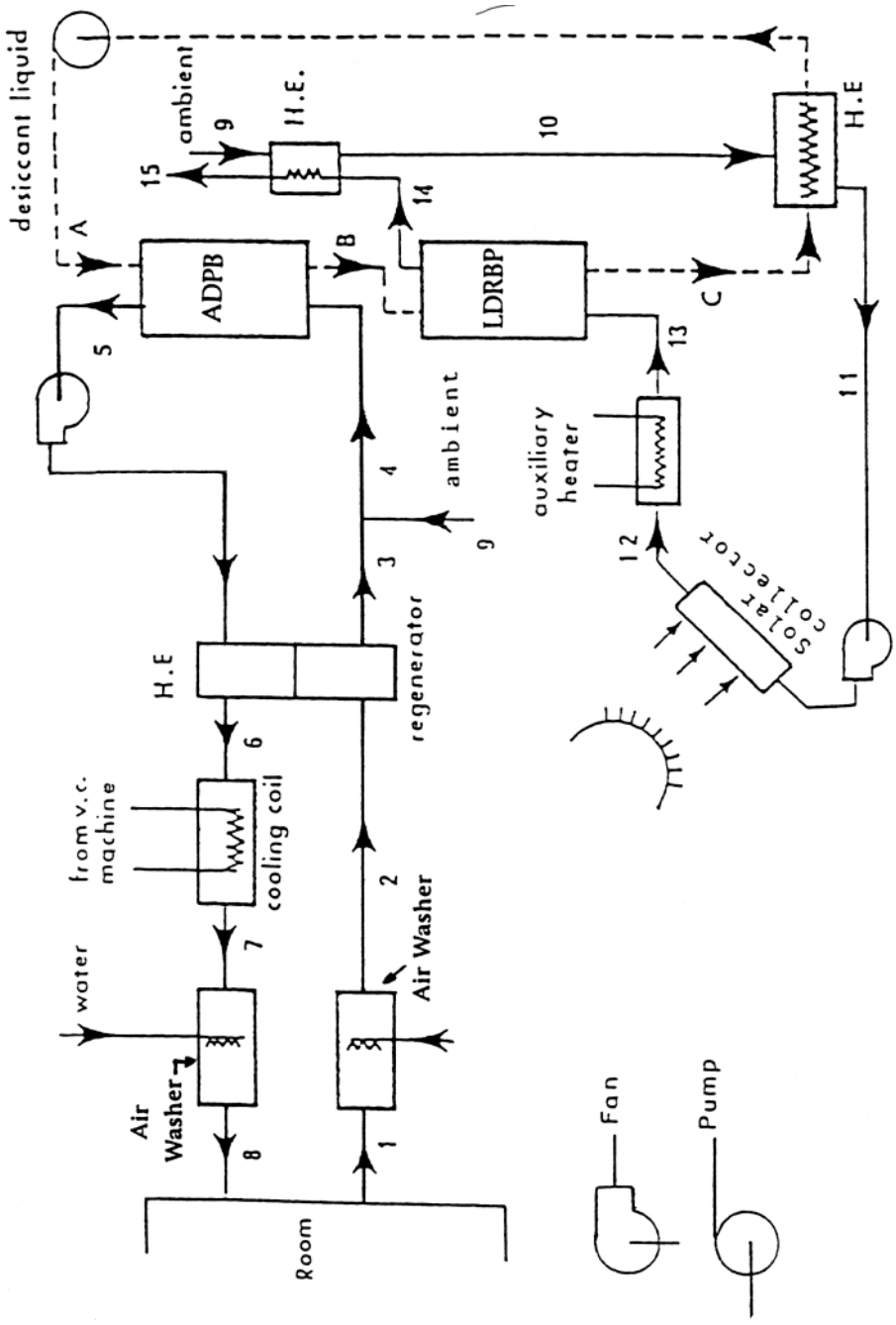

FIG. 1. The proposed solar operated, vapor compression assisted, desiccant and evaporative air conditioning system.

2. System Configuration

The system configuration, Fig. 1, is made up of three loops: the conditioned air loop, the liquid desiccant regeneration air loop, and the liquid desiccant loop.

The conditioned air loop consists of an air dehumidifier packed bed (ADPB), an air to air heat exchanger, two air humidification washers, and a cooling coil using a vapor compression refrigeration machine. The processes of the conditioned air loop are shown on the psychrometric chart, Fig. 2.

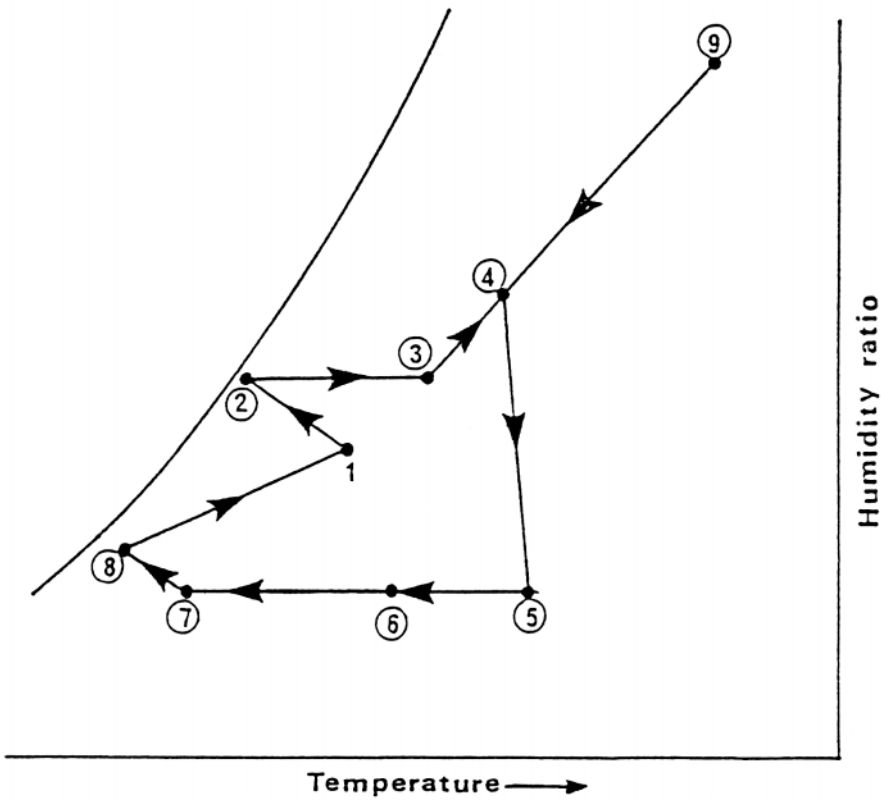

FIG. 2. The psychrometric processes of air conditioning system using vapour compression/liquid desiccant air conditioning system.

The liquid desiccant regeneration air loop consists of a liquid desiccant packed bed (LDPB), an air to air heat exchanger, an air to liquid desiccant heat exchanger, a solar air heater, and an auxiliary heater. The air process is presented on the psychrometric Chart, Fig. 3.

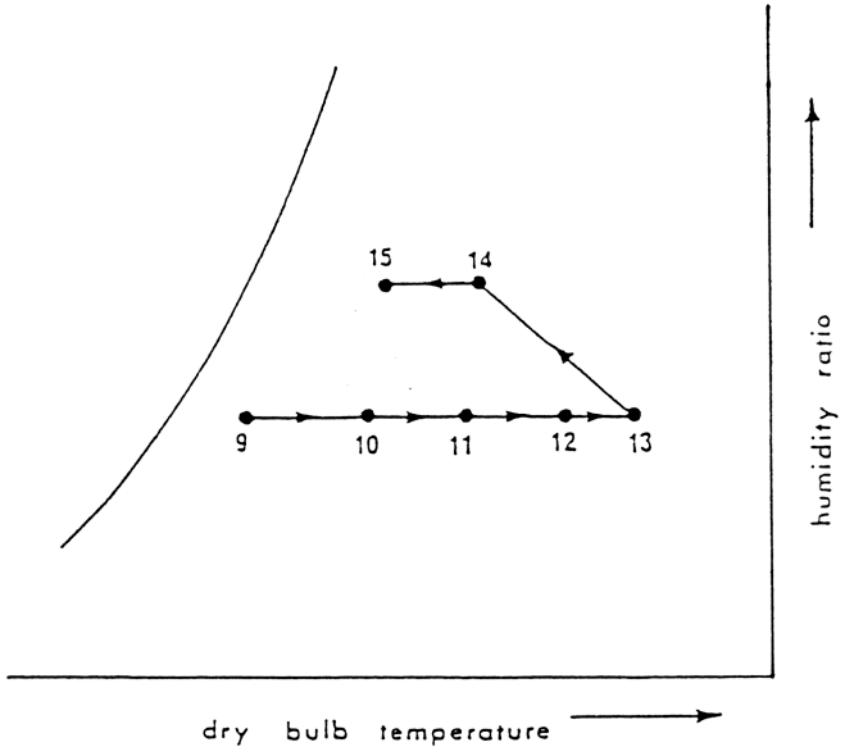

FIG. 3. Psychrometric processes for the regeneration air loop of the proposed air conditioning system.

In the liquid desiccant loop ABC, the moist liquid desiccant from the packed bed of the conditioned air loop (B) is passed to the packed bed of the liquid desiccant regeneration air loop, where it is dried to the required level (C) and recirculated back to the packed bed of the conditioned air loop. This assures a continuous supply of liquid desiccant to the conditioned air loop.

3. Modeling of Packed Beds

The mathematical modeling of both beds (ADPB) and (LDRB) are the same except for the specification of the inlet conditions of the air and liquid desiccant.

3.1 Governing equations of packed beds

The nondimensional governing equations, that are used to model the performance of the packed bed, Fig. 4, are derived in details in[15]. These equations are as follows:

$$\frac{dW}{dX} = \gamma_1 (W_\ell^* - W) \tag{1}$$

$$\frac{dY}{dX} = \gamma_2 (W_\ell^* - W) \tag{2}$$

$$(1+\gamma_4 W)\frac{dT_a}{dX}+\gamma_1\gamma_4(W_\ell^*-W)T_a=-\gamma_5(T_a-T_\ell) \tag{3}$$

$$(1+\gamma_6 Y)\frac{dT_\ell}{dX}+\gamma_2\gamma_6(W_\ell^*-W)T_\ell=(\gamma_3-\gamma_7)(W_\ell^*-W)\theta-\gamma_8(T_a-T_\ell) \tag{4}$$

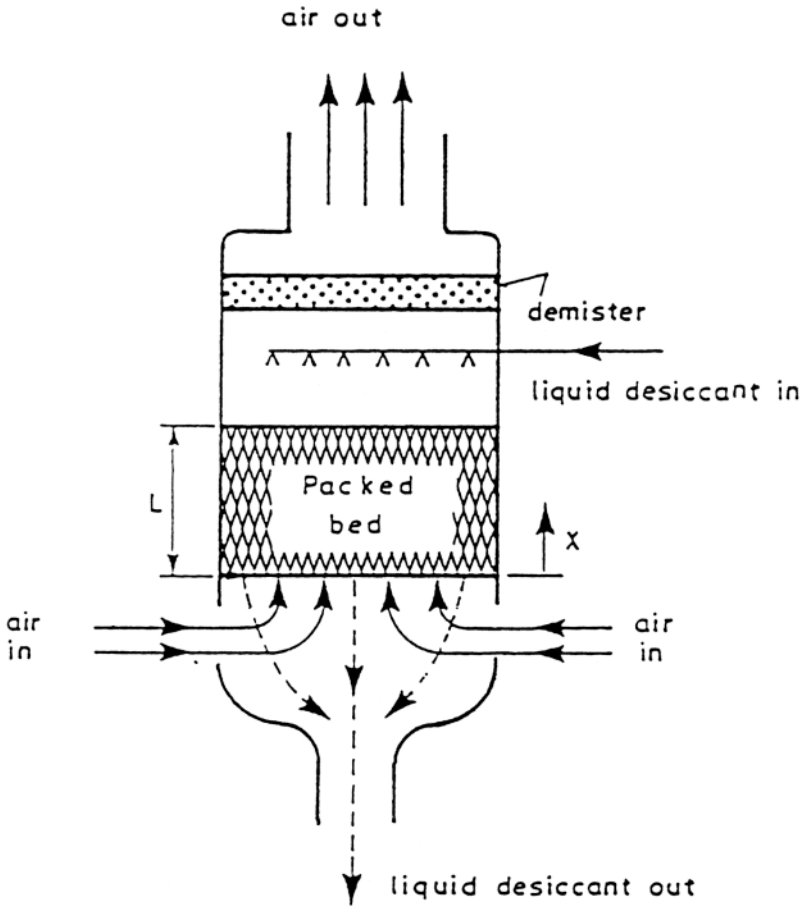

FIG. 4. Geometry of the packed bed.

and the dimensionless boundary conditions for either ADPB or LDRPB are:

$$X = 0; \qquad W = W_i, \qquad T_a = T_{ai} \tag{5}$$

$$X = 1; \qquad Y = Y_i, \qquad T_\ell = T_{\ell i} \tag{6}$$

where the following dimensionless parameters are used:

$$X = x / L \tag{7}$$

$$\gamma_1 = (\rho_a h_D A_s L) \ / \ \dot{G}'_a \tag{8}$$

$$\gamma_2 = (\rho_a h_D A_s L) \ / \ \dot{G}'_\ell \tag{9}$$

$$\gamma_3 = [(\rho_a h_D A_s L) \ / \ \dot{G}'_\ell] \ [h_{fg} / C_{p\ell}\theta)] \tag{10}$$

$$\gamma_4 = C_{pv} / C_{pa} \tag{11}$$

$$\gamma_5 = (h L A_s) / (\dot{G}'_a C_{pa}) \tag{12}$$

$$\gamma_6 = C_{pw} / C_{p\ell} \tag{13}$$

$$\gamma_7 = [(\rho_a h_D A_s L) / \dot{G}'_\ell] \ [q_b / (C_{p\ell}\theta)] \tag{14}$$

$$\gamma_8 = (h L A_s) / (\dot{G}'_\ell C_{p\ell}) W) \tag{15}$$

and θ is a reference temperature difference (assumed 10°C in the calculations). The other symbols are defined in the nomenclature list.

The governing equations (1)-(4) represent a two-point value problem. The four first order nonlinear differential equations are integrated employing a fourth order Runge-Kutta integration scheme between $X = 0$ and $X = 1$. The Nachtsheim-Swigert iteration scheme[16] is used to get T_ℓ and Y at $X = 0$. The solution is found to be stable for a wide range of operating conditions.

The properties of water, air and liquid desiccant ($CaCl_2$) at various states required for the solutions of the equations (1)-(4) and the other system components, are determined using the correlations given in ref. [17]. The bed heat transfer coefficient h, mass transfer coefficient h_D and transfer surface area A_s are calculated for Rasching Rings with 25 mm nominal diameter. Details of the calculation of these parameters and the superficial mass velocity, interfacial surface area and the modeling of heat exchangers can be found in[17,18].

4. Modeling of Air Washers

The governing equations to predict the performance of the air washer (Fig. 5) are derived in a similar way to those of liquid desiccant packed beds.

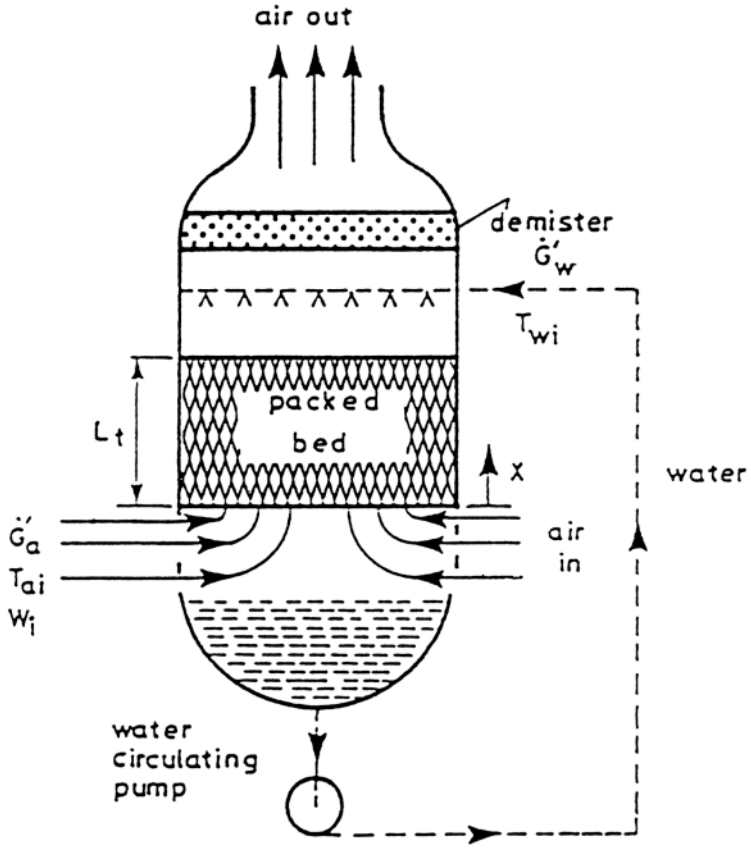

FIG. 5. Schematic drawing of an air washer.

The nondimensional form of the governing equations are written as:

$$\frac{dW}{dX_t} = \alpha_1 (W_s^* - W) \tag{16}$$

$$(1+\alpha_4 W)\frac{dT_a}{dX_t} + \alpha_1 \alpha_4 (W_s^* - W) T_a = -\alpha_5 (T_a - T_w) \tag{17}$$

$$\frac{dT_w}{dX_t} = \alpha_3 \theta (W_s^* - W) - \alpha_8 (T_a - T_w) \tag{18}$$

with the following boundary conditions:

$$\left.\begin{aligned} X_t = 0 \;;\; W = W_i \,,\; T_a = T_{ai} \\ X_t = 1 \;;\; T_w = T_{wi} \end{aligned}\right\} \tag{19}$$

The dimensionless parameters are defined as:

$$\left.\begin{aligned}
\alpha_1 &= (\rho_a h_D A_s L_t / \dot{G}'_a \\
\alpha_3 &= [(\rho_a h_D A_s L_t) / \dot{G}'_w]\ [h_{fg} / (C_{pw}\theta)] \\
\alpha_4 &= C_{pv} / C_{pa} \\
\alpha_5 &= (h L_t A_s) / (\dot{G}'_a C_{pa}) \\
\alpha_8 &= (h L_t A_s) / (\dot{G}'_w C_{pw}) \\
X_t &= x / L_t
\end{aligned}\right\} \qquad (20)$$

where W_s^* is the equilibrium humidity ratio of air in contact with the circulated water in the tower.

The same numerical schemes used to solve equations (1)-(4) are used to solve the three nonlinear first order differential equations (16)-(18) subject to one-point boundary value problem.

5. Modeling of Solar Air Heaters

Modeling of air heaters is carried out as given in[19-22] to predict the air outlet temperature.

6. Preparation of Computer Program and System Performance Calculations

A computer program LDACS (Liquid Desiccant Air Conditioning Systems) is prepared for the system in Fig. 1, using the mathematical simulation equations given in the previous sections. The program is tested by carrying out several runs at various operating conditions.

However, the preliminary testing of the computer program, based on the system configuration in Fig. 1 showed the necessity to use several heat exchangers to enhance the overall efficiency of the desiccant regeneration loop.

The results also, showed in a later stage the need to use a storage tank to store the solar thermal energy collected by the solar collectors for use at times when solar energy is not available or less than required by the system. Several bypass valves are added to the system to improve its control and to make its performance more efficient.

The modeling of the new added components was carried out in detail and can be found in[17].

The system in Fig. 1 is now modified and the final arrangement is shown in Fig. 6. To evaluate the performance of the system some parameters should be introduced.

Since the use of liquid desiccant reduces the cooling load of the vapor compression machine, one may define the desiccant replacement factor (*DRF*) as follows

$$DRF = \frac{\text{Part of cooling load replaced by the liquid desiccant system}}{\text{cooling load using only vap. comp. refrigerator}} = Q_{CLD} / Q_{CC} \quad (21)$$

where Q_{CC} is the cooling load of the vapor compression refrigerator and Q_{CLD} is the part of the cooling load which is replaced by the present liquid desiccant system.

The daily system thermal ratio (*STR)* is defined as follows:

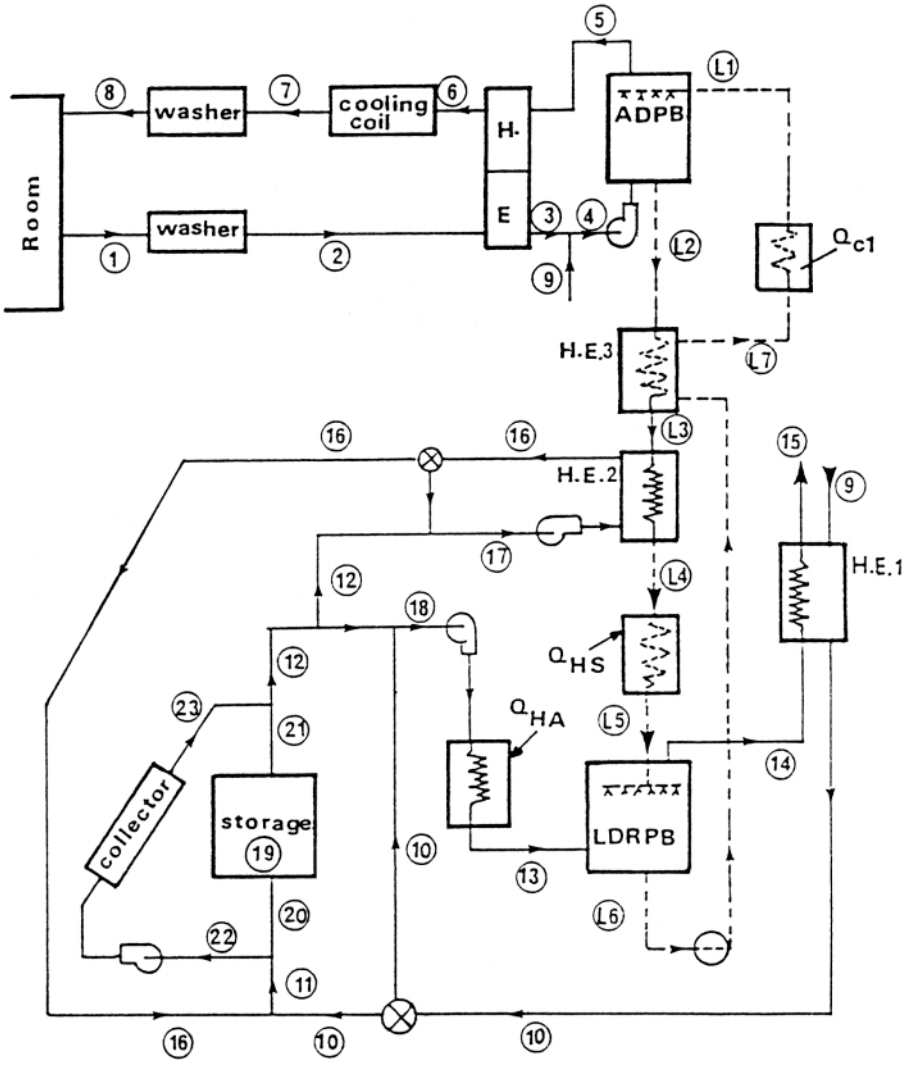

FIG. 6. Present system of air dehumidification using liquid dessicant.

$$STR = \frac{\text{daily cooling load obtained by desiccant system}}{\text{daily heat input to the system}}$$

$$STR = \left(\int_{t_1}^{t_2} Q_{CLD}\, dT \right) \Bigg/ \left(\int_{t_s}^{t_2} Q_s dt + \int_{t_1}^{t_2} (Q_{HA} + Q_{HS}) / \eta_{cd} dt \right) \tag{22}$$

where t is the solar time measured from midnight, Q_s is the solar irradiance received by the collector covers, Q_{HA} and Q_{HS} are the rate of auxiliary heat supplied to the system, and η_{cd} is the daily efficiency of solar collector. The value of η_{cd} is calculated as follows

$$\eta_{cd} = \int_{t_1}^{t_2} \dot{m}_{22} C_{pa} (T_{23} - T_{22}) dt \Bigg/ \int_{t_1}^{t_2} Q_s dt \tag{23}$$

In the above equations the time period from t_1 to t_2 is 24 hours and the starting time t_1 is any time during a day which is selected 0 for simplicity. When operating on the mean day of each month, the previous expressions for STR and η_{cd} provide directly the monthly-averaged values $\overline{STR}$ and $\overline{\eta}_{cd}$.

Similarly, the yearly-averaged daily $(STR)_y$ is defined as follows:

$$(\overline{\text{STR}})_y = \sum_{i-1}^{12} [\overline{H}_{CLD}]_i \Bigg/ \sum_{i-1}^{12} \left[\overline{H}_s + \frac{1}{\eta_{cd}} (\overline{H}_{HA} + \overline{H}_{HS} \right]_i \tag{24}$$

where $\overline{H}$ is the monthly-averaged daily value, with the subscripts *CLD*, *S*, *HA* and *HS* having the same meaning as before.

The daily solar utilization factor (*SUF*) is defined as

$$SUF = \eta_{cd} H_s / (\eta_{cd} H_s + H_{HA} + H_{HS}) \tag{25}$$

where H_s, H_{HA}, and H_{HS} are respectively the daily solar radiation received by collector surface and the daily heat energy provided by air and solution auxiliary heaters, respectively. In a similar manner to STR and $(\overline{STR})_y$, SUF and $(\overline{SUF})_y$ are defined.

7. Performance of the Overall System at Basic Design and Operating Conditions

The computer program LDACS (Liquid Desiccant Air Conditioning System) is modified to predict the transient performance of the liquid desiccant system shown in Fig. 6.

The initial values of the design and operating parameters given in the appendix are per unit area of ADPB.

7.1 Performance of the air dehumidification loop

The variation of the humidity ratio of the air flowing in the ADPB with the bed height is shown in Fig. 7. The value of W becomes almost constant at about 90% of the bed height which suggests that the height of the bed could be reduced to save the unnecessary extra initial cost of the bed without affecting the dehumidification process of the air.

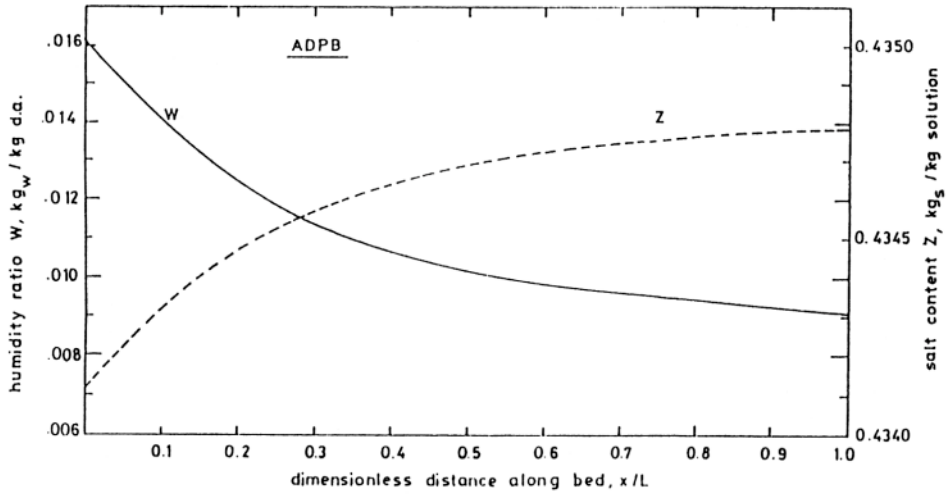

FIG. 7. Variations of humidity ratio of air and salt content in liquid desiccant flowing in the ADPB for the date of basic run.

Figure 7 also depicts the variation of the salt content Z (i.e. $CaCl_2$) in the solution with the bed height. This variation has a trend opposite to that of W.

The air dehumidification loop processes are plotted on the psychrometric chart, Fig. 8 where the state points on the figure are the same as shown in Fig. 6. The desiccant replacement factor *DRF* for the present basic run is found equal to 0.846, i.e. 84.6% of the cooling load is removed by the desiccant liquid and 15.4% of the cooling load is provided by a vapor compression refrigeration machine.

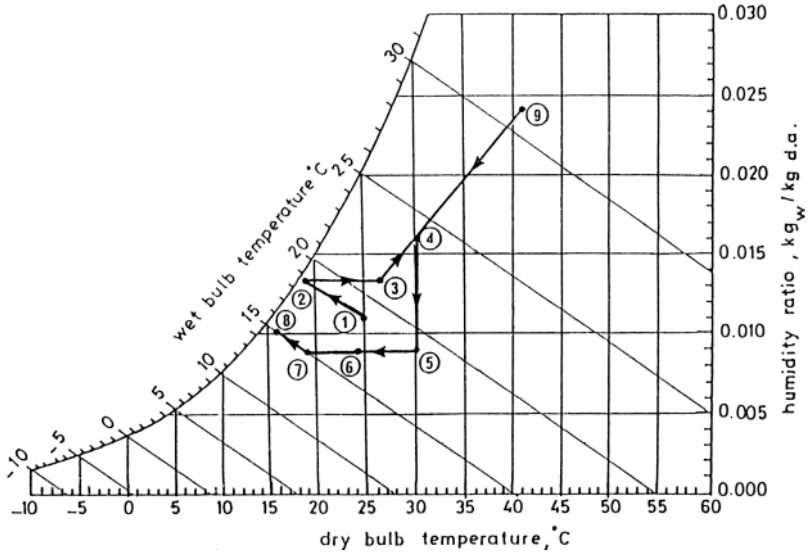

FIG. 8. Plot of air processes in the air dehumidification loop.

7.2 The liquid desiccant regeneration loop

The variations of the humidity ratio of the air and the salt content of the liquid desiccant solution, with the bed height are shown in Fig. 9.

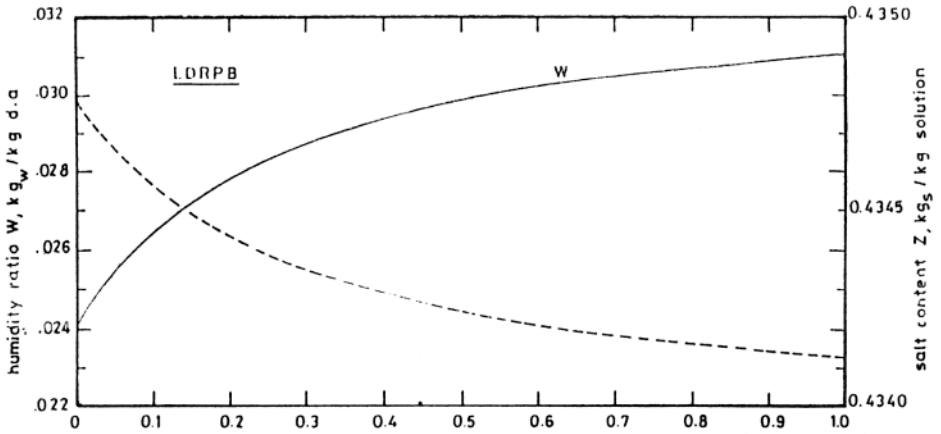

FIG. 9. Variation of humidity ratio of air and salt content in liquid desiccant flowing in the LDRPB for the data of basic run.

The time dependence of the temperatures of the air entering and leaving the solar air heater and the average rock bed temperature are shown in Fig. 10.

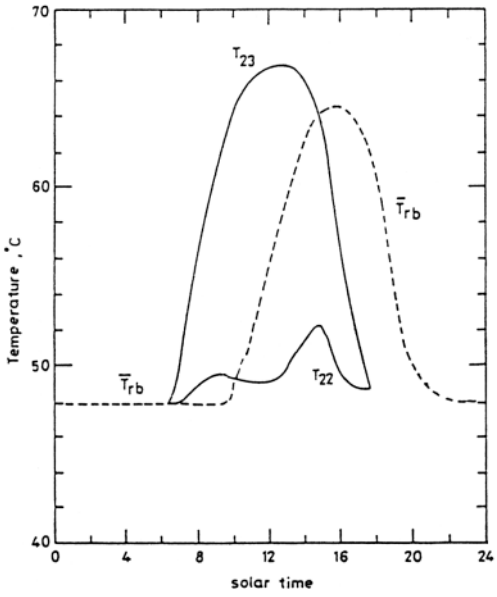

FIG. 10. Time dependence of collector inlet temperature T_{22}, collector outlet temperature T_{23}, and rock bed average temperature T_{rb} using data of basinc run.

The temperature distribution of the rock bed along the bed height is given in Fig. 11 for solar times 0, 6, 12, 18 and 24 hr.

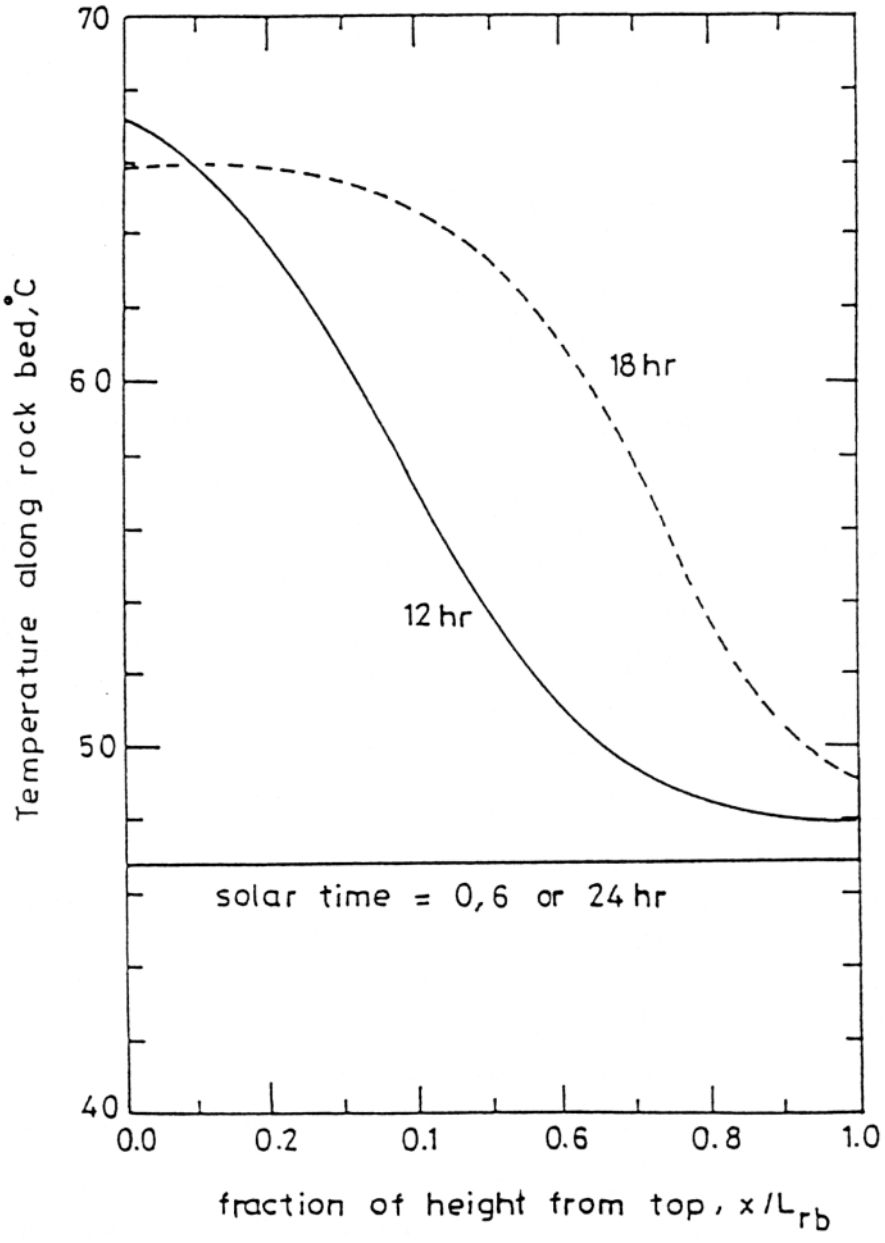

FIG. 11. Variation of temperature in rock bed along the bed height at 6, 12, 18 and 24 hr solar time using the data of basic run.

7.3 Overall performance of the system

Under the data of the basic run given in the Appendix, the performance of the system is proved to be satisfactory. All basic laws such as conservation of mass and energy equation are satisfied for all components and processes at any instant of time of the operation. The system is found to have the following:

desiccant replacement factor, *DRF*	=	0.846
system thermal ratio, *STR*	=	0.295
solar utilization, *SUF*	=	0.485

To improve the solar utilization factor a large collector area should be used, but this of course, would be on the expense of the initial cost of the system.

8. Effect of Weather Conditions on the System Performance

The system performance is now studied at the monthly-averaged daily ambient temperature and humidity ratio $\overline{T}_9$ and $\overline{W}_9$, respectively.

The results are shown in Fig. 12, and indicate that the highest value of $\overline{DRF}$ during the year is 0.825 and occurring during August and September. The lowest value of $\overline{DRF}$ is 0.74 and occurring around January. The distribution of the $\overline{SUF}$ with the months of the year is the opposite to that of $\overline{DRF}$. The high value of the $\overline{SUF}$ during January is due to the low humidity ratio of the ambient air which causes low latent cooling load and thus the present area (50 m^2/m^2 of ADPB) of solar collector becomes adequate to provide about 92% of the heat energy required to run the system. On the contrary, during August and September, the humidity ratio of the ambient air is quite high causing reasonably large value of the latent cooling load. At this large value of the latent cooling load, the present area (50 m^2/m^2 of ADPB) of solar collectors is capable of providing about 56% of the heat energy required by the system.

Examining the monthly variation of $\overline{STR}$ showed that its value varies only in a narrow range, mainly between 0.20 and 0.25. The highest value of $\overline{STR}$ is found near July (Summer) and its lowest value is found in December (Winter).

Similarly, the monthly variation of $\overline{\eta}_{cd}$ is found to be a reasonably narrow range like $\overline{STR}$. Its variation fall between 0.44 and 0.48, i.e. with 0.04 difference.

In conclusion, the results in Fig. 12 show that the performance of the system as indicated by $\overline{DRF}$ and $\overline{STR}$ is good at humid weather as that of Jeddah.

9. Effect of the Solar Collector Area

Of course, changing the area of the solar collector A_c would not affect the desiccant replacement factor *DRF* of the system. However it affects both the solar utilization factor *SUF* and the system thermal ratio *STR*.

Figure 13 depicts the variation of $\overline{SUF}$ with the ratio A_c/A_b for January (Winter) and July (Summer). It is clear that during January using $A_c/A_b \sim 60$ or more makes *SUF* = 1.0, i.e. all heating is carried out in full by solar energy. Using same value of A_c/A_b of

60 provides $\overline{SUF}$ = 0.7 during July. The yearly-averaged value of *SUF* lies between the values of January and July.

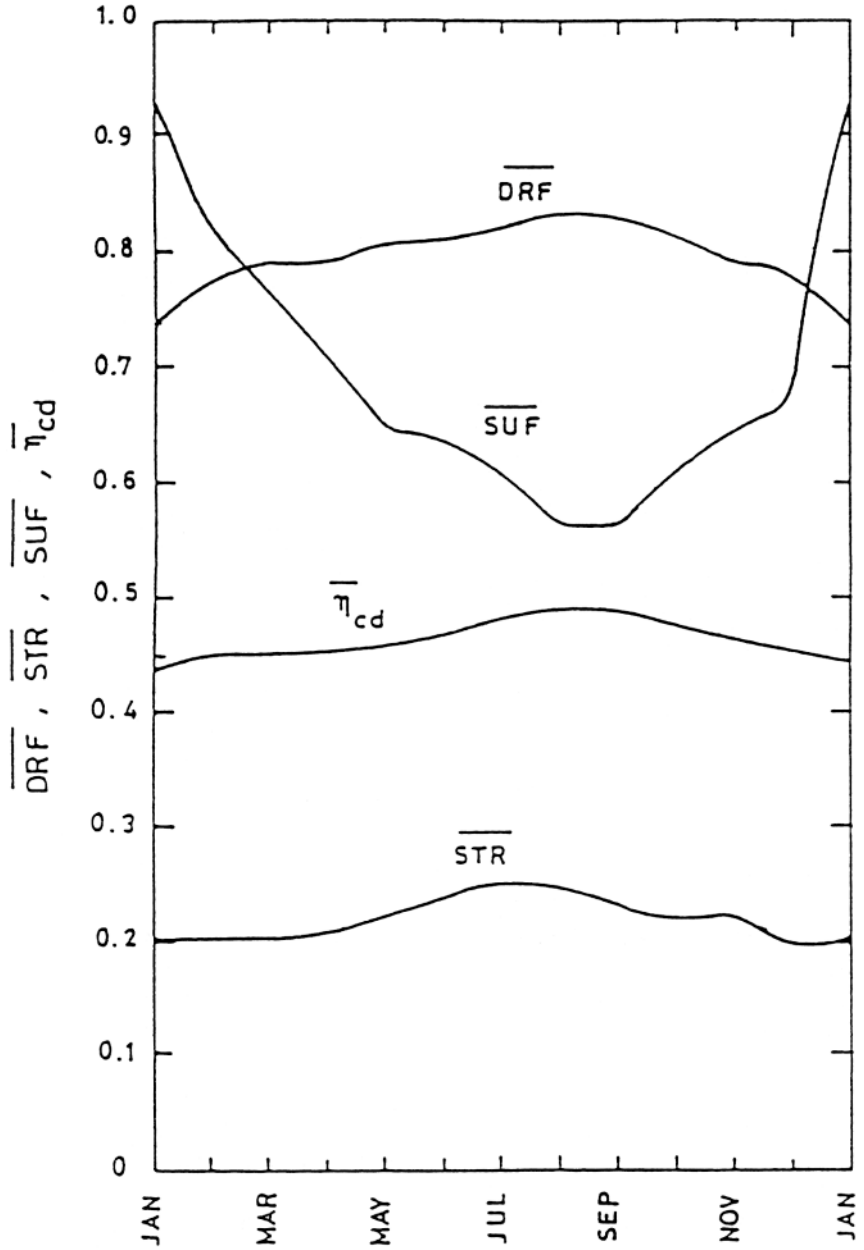

FIG. 12. The monthly variation of $\overline{DRF}$, $\overline{STR}$, $\overline{SUF}$, and $\overline{\eta}cd$.

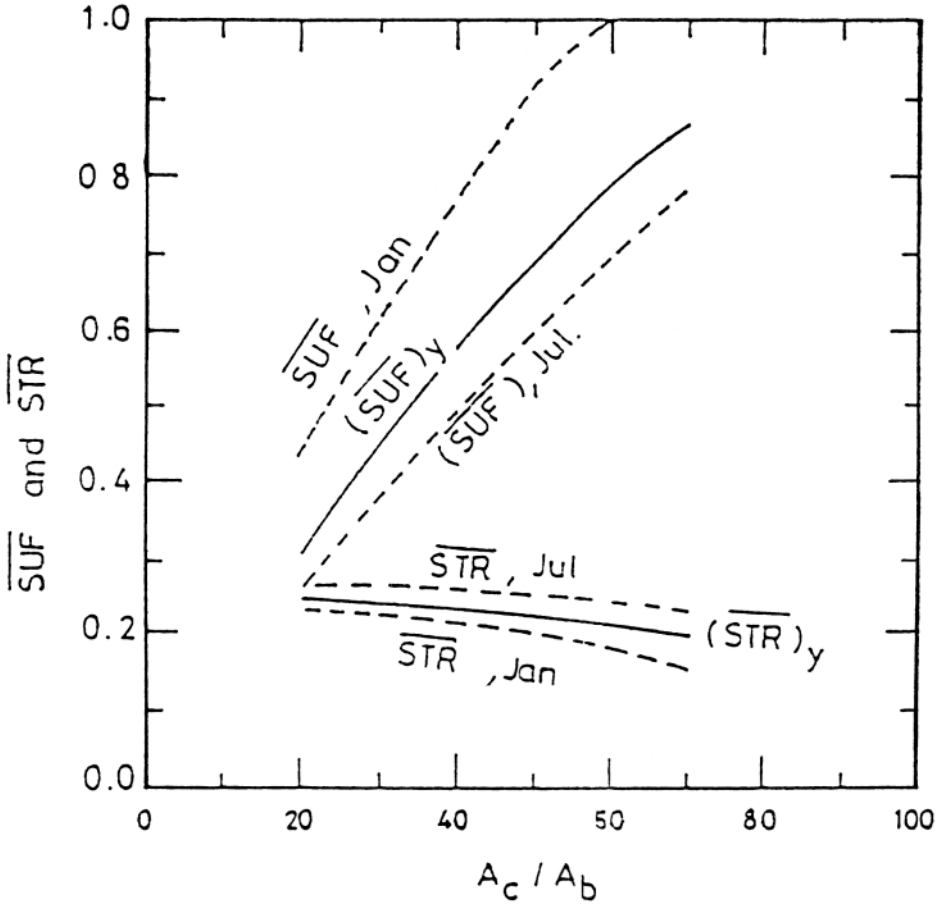

FIG. 13. Dependence of $\overline{SUF}$ and $\overline{STR}$ on the ratio A_c/A_b for the average day of January, July, and yearly average day.

Figure 13 also shows the slight change in the values of $\overline{STR}$ of January, July and the yearly-averaged day. Generally, the value of *STR* decreases as the area of collector is increased. This is expected due to the increase in the heat loss from the solar collectors as the collector area is increased. The reason is that by increasing A_c more thermal energy is supplied by the collector to the system and this makes the average temperature of the air leaving the storage tank to the collector higher during day time, and therefore more heat loss from the collectors is expected. The final conclusion is a slight drop in the collector efficiency and thus a slight drop in $\overline{STR}$ as A_c/A_b is increased.

10. Effect of the Height of the Rock Bed Thermal Storage

The effect of changing the height of the rock bed thermal storage on the long-term performance of the system is considered. Bed heights of 1, 2, 3, and 4 m are studied

with the other design and operating conditions held constant as given in the Appendix and using the weather data for Jeddah[23].

Figure 14 presents the variation of the $\overline{SUF}$ and $\overline{STR}$ of the system for the average day of January, July, and the year with the rock bed height L_{rb} for the same area of solar collectors. Increasing the rock bed heights means using large volume of rock bed to store the surplus thermal energy collected by solar collectors. This leads to reducing the input air temperature to the collector, thus improving the collector efficiency, and as a result also improving $\overline{SUF}$. The improvement in $\overline{SUF}$, however, diminishes as L_{rb} is increased, and it becomes negligible as L_{rb} is increased beyond 3 m. Similarly, $\overline{STR}$ is improved with the increase in L_{rb} due to the improvement of the efficiency of the solar collectors as explained before.

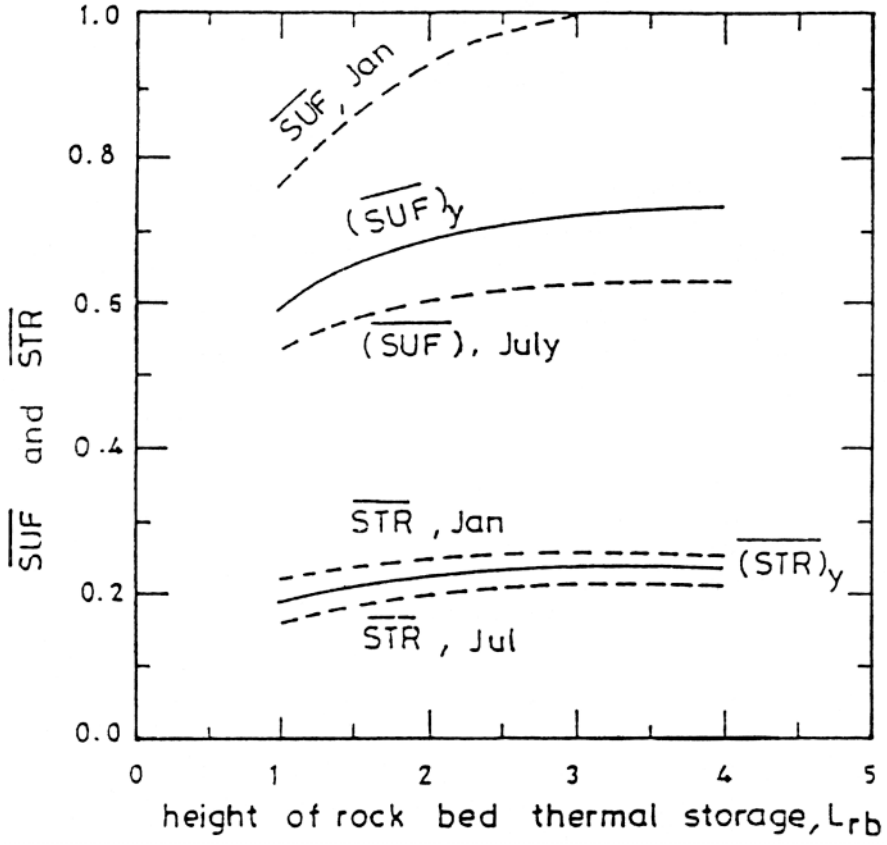

FIG. 14. Dependence of $\overline{SUF}$ and $\overline{STR}$ on L_{rb} for the average day of January, July and the year.

11. Conclusions

A mathematical model is prepared to simulate the performance of the integrated solar operated, vapor compression assisted, liquid desiccant air conditioning system. Three

indices: *DRF*, *STR*, and *SUF* are introduced to evaluate the performance of the system at various design and operating conditions.

A FORTRAN computer package LDACS is prepared, and extensively tested, using the present mathematical model. The package is also used to predict the long-term performance of the system when operated at the weather data of Jeddah. In addition, the package is used to study the long-term performance of the system when changing the area of the solar collectors and the height of the thermal storage tank. The package may be used to predict the performance of the present system at other parametric conditions and thus helps to optimize the system.

Acknowledgement

The present work is funded by the Research Administration of King Abdulaziz University (Grant No. 039/411).

List of Symbols

A_b	cross sectional area of ADPB, m^2.
A_c	area of solar collectors.
A_s	heat transfer and mass transfer area in packed bed, m^2/m^3.
C_p	specific heat at constant pressure, J/kg ^oC.
DP	Dew Point.
DRF	desiccant replacement factor.
G	solar irradiance, W/m^2.
$\dot{G}'_a$	superficial mass velocity of dry air in packed bed, kg_{da}/m^2 s.
$\dot{G}'_c$	mass of air flow rate in solar collector per unit cross sectional area of ADPB, kg/m^2·s.
$\dot{G}'_\ell$	superficial mass velocity of salt in liquid desiccant flowing in packed bed, kg_s/m^2·s.
h	heat transfer coefficient in packed beds, W/m^2 ^oC, also, enthalpy of air, J/kg.
H	monthly-averaged daily total radiation on a horizontal plate.
h_D	mass transfer coefficient, m/s.
h_{fg}	latent heat of evaporation for water, J/kg.
k	thermal conductivity.
L	height of packed bed.
L_t	height of packed bed of air washer.
m	flow rate, kg/s.
$\dot{m}$	mass flow rate per unit cross sectional area of ADPB, kg/m^2·s.
P_{ws}	saturation pressure of water at a given temperature, kPa.
Q	rate of heat transfer.
Q_{CLD}	part of cooling load provided by liquid desiccant system, W.
Q_{HA}	rate of heat supplied to the auxiliary air heater, W.
Q_{HS}	rate of heat supplied to the auxiliary solution heater, W.
s	tilt angle of solar collector.
STR	daily system thermal ratio.
SUF	solar utilization factor.

t	time, also solar time.
T	temperature, ºC.
W	humidity ratio of air, kg_w/kg dry air.
X	dimensionless distance.
x	distance along packed bed, m. also, mole fraction of water in liquid desiccant.
Y	moisture content in liquid desiccant, dry base, kg H_2O/kg salt.
y	mole fraction of water vapor in air.
Z	salt content in liquid desiccant, kg salt/kg solution.

Greek Symbols

α	absorptance of absorber plate of solar collector.
α_1 to α_8	dimensionless coefficients, Eqn (20).
γ_1 to γ_8	dimensionless coefficients, see eqs. (7) to (15).
ε	effectiveness of a heat exchanger.
η	efficiency of solar collector.
η_{cd}	daily thermal efficiency of the solar collector.
θ	reference temperature difference (assumed 10ºC in calculations); also, solar incidence angle on a tilted surface.
μ	dynamic viscosity, Pa.s.
ρ	density, kg/m^3; also reflectance.
ϕ	relative humidity of air; also latitude angle.

Superscripts

*	equilibrium conditions.
′	superficial.
.	rate.

Subscripts

1,2	state point of air.
a	air.
c	cold fluid.
DP	Dew Point.
gr	ground reflected.
h	hot fluid.
i	inlet condition;
ℓ	liquid desiccant.
l	liquid.
*L*1,*L*2	State point of liquid desiccant.
o	out.
rb	rock bed.
s	saturation condition of air; also, solution (water or liquid desiccant solution); also, salt; also; solar.
t	on a tilted surface.
v	water vapor.

w water.
∞ ambient.

References

[1] **Lof, G.O.G.,** House heating and cooling with solar energy. *Solar Energy Research, University of Wisconsin, Madison* (1955).

[2] **Kapur, J.C.,** A report on the utilization of solar energy for refrigeration and air-conditioning applications. *Solar Energy* **5:** 39 (1960).

[3] **Mitchell, W.,** State of the art of active solar cooling. *Proceedings ASES* 86, Annual Meeting, N.Y., pp. 59-71 (1986).

[4] **Schultz, K.J.** and **Mitchell, J.W.,** Performance of solar-desiccant systems using cooled desiccant beds. *ASES,* Knowville, Tennessee, U.S.A. (1982).

[5] **Jurinak, J.J., Mitchel, J.W.** and **Beckman, W.A.,** Open-cycle desiccant air-conditioning as an alternative to vapor compression cooling in residential applications. *J. Solar Energy* **106:** 252-260, August (1984).

[6] **Beba, S., Cles, G.** and **Lof, G.,** Performance of a solar desiccant cooling system. *Proceedings of ISES* 86 Annual meeting, International Conference on High Power Particle Beams, Kobe, Japan (1986).

[7] **Joudi, K.** and **Madhi, M.,** An experimental investigation into a solar assisted desiccant-evaporative air-conditioning system. *J. Solar Energy* **39:** 97-107 (1987).

[8] **Johannsen, A.,** Design and operation of liquid desiccant type solar A/C system. *Proceedings of International Solar Energy Society (ISES),* Atlanta, GA, pp. 681-685 (1979).

[9] **Buschulte, T.K.** and **Klein, S.A.,** Analysis of a hybrid liquid desiccant cooling system. *Biennial Congress of the International Solar Energy Society (ISES),* Intersol 85 Conference, Montreal, Quebec (1985).

[10] **Johannsen, A.,** Performance simulation of solar A/C system with liquid desiccant. *Int. J. Ambient Energy* (U.K.) **5** (1984).

[11] **Lof, G.,** *et al.* Design and testing of solar cooling systems employing liquid desiccants. *Final Report of Contract* DE-FG03-SF1306, Colorado State University, Ft. Collins, December (1987).

[12] **Gandhidasan, P.,** Potential Use of Liquid Desiccants in Solar Applications, *Proc. of ISES Solar World Congress 1989,* Kobe, Japan, pp. 4-8, Sept. (1989).

[13] **Patnaik, S., Lenz, T.G.** and **Lof, G.O.,** Performance Studies on an Experimental Solar Open-Cycle Liquid Desiccant Air Dehumidification System, *Solar Energy,* **44**(3): 123-135 (1990).

[14] **Gandhidasan, P.,** Analysis of a Solar Space Cooling Systems Using Liquid Desiccants, ASME Trans. *J. of Energy Resources Tech.,* **112**(4): 246-250, Dec. (1990).

[15] **Radhwan, A.M., Gari, H.N.** and **Elsayed, M.M.,** Parametric Study of a Packed Bed Dehumidification/ Regenerator Using $CaCl_2$ Liquid Desiccant, *Renewable Energy,* **3**(1): 49-60 (1993).

[16] **Adams, J.A.** and **Rogers, D.F.,** *Computer-Aided Heat Transfer Analyses.* McGraw-Hill, New York (1973).

[17] **Radhwan, A.M., Gari, H.N.** and **Elsayed, M.M.,** Experimental investigation of a packed bed for liquid desiccant solar cooling system. Final Report of Project No. 039/411, Scientific Research Administration, King Abdulaziz University, Jeddah, Saudi Arabia (Jan. 1993).

[18] **Treybal, R.E.,** *Mass Transfer Operations,* McGraw-Hill Book Company, N.Y. (1980).

[19] **ASHRAE,** ASHRAE Handbook of HVAC Applications (1991).

[20] **Elsayed, M.M., Fathallah, K.A.** and **Megahid, I.A.,** *Mathematical Modeling of Solar Thermal Systems,* King Abdulaziz University (1988). *In Arabic.*

[21] **Elsayed, M.M.,** Optimum Orientation of Absorber Plates, *Solar Energy,* **42**: 89-102 (1989).

[22] **Duffie, J.** and **Beckman, W.A.,** *Solar Engineering of Thermal Process,* John Wiley & Sons, N.Y. (1980).

[23] **Annual Environmental Report,** General Directorate of Meteorology, Saudi Arabia (1990).

Appendix

Basic design and operating conditions of the present liquid desiccant air conditioning system.

A. Room and Ambient Conditions

A1.	Dry bulb temperature, T_1	=	25ºC
A2.	Humidity ratio, W_1	=	0.011 $kg_w/kg_{d.a.}$
A3.	Air flow to room per m^2 of cross section area of ADPB	=	0.45 $kg/s{\cdot}m^2$
A4.	Ambient dry bulb temperature, T_9	=	41ºC
A5.	Ambient humidity ratio, W_9	=	0.024 $kg_w/kg_{d.a.}$
A6.	Fraction of fresh air mixed with state 3	=	0.25

B. Air Washer

B1.	Packing material	=	Ceramic Rasching rings, 25 mm nominal diameter.
B2.	Height of bed	=	1 m
B3.	Air flow rate per unit cross sectional area of bed	=	0.45 $kg/s{\cdot}m^2$
B4.	Water flow rate per unit cross sectional area of bed	=	0.9 $kg/s{\cdot}m^2$

C. The Air Dehumidification Packed Bed, ADPB

C1.	Packing material	=	Ceramic Rasching rings, 25 mm nominal diameter.
C2.	Bed height	=	0.75 m
C3.	Air flow rate per unit cross sectional area of bed	=	0.45 $kg/s{\cdot}m^2$
C4.	Solution (liquid) flow rate per unit cross sectional area of bed	=	0.9 $kg/s{\cdot}m^2$
C5.	Solution temperature at bed inlet, T_{L1}	=	30ºC
C6.	Solution concentration at bed inlet, T_{L1}	=	1.3 kg_w/kg salt

D. Other Data for the Air Dehumidification Loop

D1.	Dry bulb temperature of supply air to the room, T_8	=	15.0ºC
D2.	Humidity ratio of supply air to the room, W_8	=	0.0106 $kg_w/kg_{d.a.}$
D3.	Effectiveness of heat exchanger between processes 2-3 and 5-6	=	0.7

E. Liquid Desiccant of Regeneration Packed Bed, LDRPB

E1.	Packing material	=	Same as C1
E2.	Bed height	=	Same as C2
E3.	Air flow rate per unit cross sectional area of bed	=	Same as C3
E4.	Solution (liquid) flow rate per unit cross sectional area of bed	=	Same as C4
E5.	Solution temperature entering the bed, T_{L5} is controlled to maintain Y_{L6}	=	Y_{L1}

F. Solar Air Heaters (Collectors)

F1.	Collector area per unit cross section area of ADPB, A_c/A_b	=	50 m^2
F2.	Collector air flow rate per unit area of collector, $\dot{G}_c'$	=	0.03 $kg/s{\cdot}m^2$
F3.	Latitude angle of Jeddah, ϕ	=	21.5º
F4.	Day of testing	=	June 21

G. Rock Bed Thermal Storage Tank

G1.	Cross sectional area per unit area of solar collector, A_{rb}/A_c	=	0.075
G2.	Average diameter of rocks	=	0.025 m (25 mm)
G3.	Voidage of the rock bed	=	0.4
G4.	Bed height	=	2.0 m
G5.	Density of Rocks	=	2640 kg/m^3
G6.	Heat capacity of rocks	=	840 J/kg ºC

H. Other Data for the Solution Regeneration Loop

H1.	Effectiveness of heat exchanger #1, ε_1	=	0.7
H2.	Effectiveness of heat exchanger #2, ε_2	=	0.8
H3.	Effectiveness of heat exchanger #3, ε_3	=	0.75
H4.	Air temperature to the LDRPB, T_{13}	=	T_{L5}
H5.	Ratio of air flow rate to H.E. 2 to that of the ADPB, m_{17}/m_4	=	3.0

النمذجة الرياضية لنظام تكييف هواء بطريقة سائل التجفيف وتشغيله بالطاقة الشمسية

عبد الحي محمد رضوان* ، مصطفى محمد السيد و هداية اللّه قاري***

** قسم الهندسة الميكانيكية ، جامعة الملك عبد العزيز ، جدة – المملكة العربية السعودية*

*** قسم الهندسة الميكانيكية ، جامعة الكويت ، الصفاة – الكويت*

المستخلص . تم إعداد نموذج رياضي لنظام تكييف هواء بطريقة التجفيف بواسطة سائل تجفيف وتشغيله بواسطة الطاقة الشمسية ، وقد جرى تطوير النظام عدة مرات للوصول إلى أداء أفضل ، ولتقويم أداء النظام تم تعريف ثلاثة عوامل (أدلة) : عامل إحلال التجفيف (DRF) ، النسبة الحرارية للنظام (STR) ، وعامل استخدام الطاقة الشمسية (SUF) . وباستخدام هذه العوامل جرى دراسة أداء نظام تكييف الهواء تحت ظروف ومناخ مدينة جدة ، إضافة إلى دراسة تأثير تغير مساحة المجمعات الشمسية وارتفاع خزان التخزين الحراري على النظام المقترح .

وقد أظهرت النتائج أن المعدل الشهري للقيمة اليومية للمعامل (DRF) تصل إلى أقصى قيمة خلال فصل الصيف وأدنى قيمة خلال فصل الشتاء . وقد أظهر المعامل (SUF) قيمًا معاكسة للمعامل (DRF) ، بينما لوحظ أن التغيير الشهري للكفاءة والمعامل (STR) كان طفيفًا خلال فصول السنة . وقد أوضحت نتائج البحث أن أداء النظام المقترح يكون جيداً في الأجواء المناخية الرطبة .